Density functional studies on the exchange interaction of a dinuclear Gd(III)–Cu(II) complex: method assessment, magnetic coupling mechanism and magneto-structural correlations†

Gopalan Rajaraman,* Federico Totti, Alessandro Bencini, Andrea Caneschi, Roberta Sessoli and Dante Gatteschi

Received 7th October 2008, Accepted 13th January 2009
First published as an Advance Article on the web 13th March 2009
DOI: 10.1039/b817540c

Density functional calculations have been performed on a [Gd(III)Cu(II)] complex $[L^1CuGd(O_2CCF_3)_3(C_2H_5OH)_2]$ (**1**) (where L^1 is *N*,*N*′-bis(3-ethoxy-salicylidene)-1,2-diamino-2-methylpropanato) with an aim of assessing a suitable functional within the DFT formalism to understand the mechanism of magnetic coupling and also to develop magneto-structural correlations. Encouraging results have been obtained in our studies where the application of B3LYP on the crystal structure of **1** yields a ferromagnetic *J* value of –5.8 cm^{-1} which is in excellent agreement with the experimental value of –4.42 cm^{-1} ($\hat{H} = J\hat{S}_{Gd}\cdot\hat{S}_{Cu}$). After testing varieties of functional for the method assessment we recommend the use of B3LYP with a combination of an effective core potential basis set. For all electron basis sets the relativistic effects should be incorporated either *via* the Douglas–Kroll–Hess (DKH) or zeroth-order regular approximation (ZORA) methods. A breakdown approach has been adopted where the calculations on several model complexes of **1** have been performed. Their wave functions have been analysed thereafter (MO and NBO analysis) in order to gain some insight into the coupling mechanism. The results suggest, unambiguously, that the empty Gd(III) 5d orbitals have a prominent role on the magnetic coupling. These 5d orbitals gain partial occupancy *via* Cu(II) charge transfer as well as from the Gd(III) 4f orbitals. A competing 4f–3d interaction associated with the symmetry of the complex has also been observed. The general mechanism hence incorporates both contributions and sets forth rather a prevailing mechanism for the 3d–4f coupling. The magneto-structural correlations reveal that there is no unique parameter which the *J* values are strongly correlated with, but an exponential relation to the *J* value found for the O–Cu–O–Gd dihedral angle parameter is the most credible correlation.

1. Introduction

High spin molecules, notably those which behave as a single molecule magnets (SMMs) continue to be of intense interest due to their potential applications.[1] An exceedingly large number of the SMMs reported to-date contain transition metal atoms but only recently this class of compounds has also embraced the presence of lanthanide ions.[2] In particular, the combination of 3d and 4f elements to form large cluster aggregates has produced several novel SMMs with attractive blocking temperatures and thus a slow relaxation of magnetisation.[3,4] The immediate advantage of the 4f elements are the large spin and pronounced spin–orbit coupling resulting in large Ising type anisotropy and, therefore, even small nuclearity (tri, tetra, penta *etc.*) complexes exhibit very large blocking temperatures.[3]

Like in transition metal chemistry, the magnetic exchange interaction plays a crucial role in the determination of spin ground state in 3d–4f type complexes. Despite extensive experimental data there are only a few reports[5–7] on the theoretical side particularly on the evaluation of the magnetic exchange *J*. This is particularly important as it offers a unique methodology which can then be extended to much larger and intriguing systems such as polynuclear single molecule magnets or single chain magnets containing a mixture of 3d–4f or 4f radical building blocks.

We have chosen here an archetypal binuclear 3d–4f Gd(III)–Cu(II) complex to perform DFT calculations.[8] The 4f ion, Gd(III), has an orbitally non-degenerate ground state and exhibits dominant isotropic interaction, which makes it simple to handle within the framework of DFT calculations. The comprehensive experimental studies on several [GdCu] complexes suggest that the exchange interaction between the Cu(II) and the Gd(III) is often ferromagnetic but some exceptions where this interaction is antiferromagnetic are also reported.[9] Apart from obtaining the right sign and good numerical estimate of the *J* constant, the importance of DFT calculations is to get insights into the mechanism of magnetic coupling between the two ions. The energy ordering of the magnetic orbitals of the Gd(III) and those belonging to the Cu(II) is very different and this presents a non-trivial coupling mechanism. Although an extensive CASSCF study on the [GdCu] unit reported earlier[5] presents several useful hints and insights on the coupling mechanism, we have tackled this issue using the DFT wave function and aim to obtain further clues on the coupling. We also finally stress here that thorough understanding of the mechanism is important for studies on

Università degli Studi di Firenze, INSTM, Polo Scientifico, Dipartimento di Chimica, via della Lastruccia 3, 50019, Sesto F.no, Italy. E-mail: gopalan.rajaraman@gmail.com

† Electronic supplementary information (ESI) available: MO models of **1c**, bond orbital coefficients of **1**, experimental *J* values and discussion of DFT functionals. See DOI: 10.1039/b817540c

higher nuclearity complexes and also for predicting the expected magnetic properties of new molecules. Another important issue which has not been addressed so far from the theoretical side is the magneto-structural correlation, despite the presence of two experimental correlations[10,11] and numerous experimental data on-hand for the [GdCu] unit. To this end we have studied the binuclear complex[8] $[L^1CuGd(O_2CCF_3)_3(C_2H_5OH)_2]$ (where L^1 is *N*,*N*′-bis(3-ethoxysalicylidene)-1,2-diamino-2-methylpropanato) with state-of-the-art DFT methods and also performed calculations on several model complexes to obtain insights into the coupling mechanism. We have also developed magneto-structural correlations for the *J* values and the Cu–O–Gd angle (or Cu···Gd distance) and the O–Cu–O–Gd dihedral angle.

2. Computational details

The magnetic exchange interaction between the Gd and the Cu ion is described by the following spin Hamiltonian,

$$\hat{H} = J\hat{S}_{Gd}\hat{S}_{Cu}.$$

Here *J* is the isotropic exchange coupling constant and S_{Gd} and S_{Cu} are the spins on the gadolinum(III) ($S = 7/2$) and the copper(II) ($S = 1/2$) centers, where negative *J*'s correspond to ferromagnetic interaction. To compute the *J* values one has to compute the energies of the high spin state ($S_T = 4$) and the one of the low spin state ($S_T = 3$). The energy of the high spin state can be computed straightforwardly using a single determinant wave function such as DFT methods. However for the low spin state some approximations are required due to its multi-determinantal characteristics. Thanks to the broken symmetry model developed by Noodleman[12] which has been widely used[13] and provides a good approximation to the energy of the low spin state (also called broken symmetry state), one can compute *J* values using HF or DFT calculations. For heterobinuclear transition metal complexes the following equation has been advocated:[14]

$$J = \frac{E_{BS} - E_{HS}}{2S_{Gd}S_{Cu}}$$

where *J* is the isotropic magnetic exchange interaction, E_{BS} and E_{HS} are the energies of the broken symmetry and the high spin state respectively. All the computations were performed using the JAGUAR suite of programs[15] with a combination of a hybrid B3LYP[16] functional with a double zeta quality basis set employing Cundari–Stevens (CS) relativistic effective core potential (ECP) (named CSDZ in JAGUAR) on the Gd[17] and a Los Alamos ECP, LanL2DZ on the Cu[18] and the popular 6-31G[19] on the rest of the elements unless otherwise mentioned. In the ECP treatment, the core electrons are modelled using a suitable function and only the valence electrons are treated explicitly. The relativistic effects are vital for the rare earth ions and by employing the ECP basis set the scalar relativistic components are incorporated indirectly in the calculations. The CSDZ basis set uses ECP for the inner core of the Gd and treats the outer core and valence electrons with a 4s/4p/2d/2f basis set. For the basis set dependency tests several combinations of basis sets have been employed particularly for the metal ions. For Cu, a triple zeta quality basis set termed LanL2TZ(f),[20–22] the Stuttgart ECP basis set termed SDD,[23,24] the Ermler and co-workers CRENBL basis set,[25–26] the all electron basis set of Alrichs[27] and co-workers (SVP and TZVP) and an all electron Wachters[28] and co-workers basis set have been used. For the Gd, CS ECP, CRENBL, SDD and an all electron basis set of Nakajima and co-workers[29] have been employed. The all electron calculations have been performed by incorporating the relativistic effects either *via* the zeroth-order regular approximation[32] (ZORA) or *via* the Douglas–Kroll–Hess (DKH)[30,31] method. The basis set tests have been done with the Gaussian 03[33] and the ORCA[34] suites of programmes. A very tight SCF (self consistent field) convergence of 5×10^{-8} for the total energy has been employed in order to obtain more precise *J* values. The $<S^2>_{HS}$ and $<S^2>_{BS}$ values obtained for different functionals and basis sets are given in Tables 1 and 2 and only very little deviation from the expected values has been observed.

Table 1 DFT computed *J* values with different functionals and CSDZ basis set

Functional	J/cm^{-1}	$<S^2>$ (HS, BS)	Spin density on (Gd, Cu) on $S = 4$ state	% of HF exchange
Exp	−4.42			
BLYP	−7.0	20.011, 13.011	(7.022, 0.508)	0%
HCTH	−8.8	20.023, 13.022	(6.999, 0.462)	0%
B3LYP	−5.9	20.013, 13.013	(7.022, 0.508)	20%
B3P86	−6.3	20.014, 13.014	(7.032, 0.592)	20%
B97–1	−6.8	20.016, 13.016	(7.007,0.621)	21%
X3LYP	−5.8	20.013, 13.013	(7.022, 0.606)	21.8%
B98	−7.9	20.018, 13.013	(6.873,0.595)	21.98%
SB98	−6.6	20.016, 13.016	(7.011,0.6223)	21.98%
MPW1PW91	−5.8	20.015, 13.015	(7.032, 0.623)	25%
BHandH	−3.6	20.026, 13.026	(7.052, 0.724)	50%
BHandHLYP	−3.8	20.021, 13.021	(7.052, 0.719)	50%

Table 2 DFT computed *J* values with the B3LYP functional and different basis sets

Basis set	J/cm^{-1}	$<S^2>$ (HS, BS)	Description	Relativistic
CSDZ	−5.8	20.011, 13.011	Cu (LanL2DZ ECP), Gd (CS ECP) and others (6–31G)	ECP
CSDZ*	−5.8	20.013, 13.013	Cu (LanL2DZ ECP), Gd (CS ECP) and others (6–31G*)	ECP
BS III	−5.7	20.014, 13.001	Cu (LanL2TZ(f)[21,22] ECP), Gd (CS ECP) and others (6–31G)	ECP
BS IV	−5.9	20.010, 13.010	Cu (SDD[24] ECP), Gd (SDD[24] ECP) and others (6–31G)	ECP
BS V	−5.5	20.014, 13.014	Cu (LanL2TZ(f) ECP), Gd (CS ECP) and others (6–311++G**)	ECP
BSVI	−5.2	20.008, 13.008	Cu (CRENBL[25,26] ECP), Gd (CRENBL ECP) and others (6–31G)	ECP
BS VII	−7.5	20.008, 13.006	Cu (SVP), Gd (Nakajima[29] all e$^-$) and others (SVP)	None
BS VIII	−7.2	20.008, 13.006	Cu (TZVP), Gd (Nakajima all e$^-$) and others (SVP)	None
BS VIII-R	−5.8	20.007, 13.006	Cu (TZVP), Gd (Nakajima all e$^-$) and others (SVP)	DKH2
BS IX-R	−5.8	20.007, 13.006	Cu (Watchers[28] all e$^-$), Gd (Nakajima all e$^-$) and others (SVP)	DKH2
BS X-R	−5.7	20.007, 13.006	Cu (TZVP), Gd (Nakajima all e$^-$) and others (SVP)	ZORA

3 Results and discussion

3.1 Exchange interaction in binuclear $[L^1CuGd(O_2CCF_3)_3(C_2H_5OH)_2]$

The density functional theory studies on rare earth compounds are seemingly difficult unlike in the transition metal compounds as the unpaired electron on the rare earth atoms is very low in energy compared to that of the ligand orbitals and the transition metal d-orbitals, thus posing a challenge to convergence of the wave function to a well-defined electronic ground state. The computation of the J values using DFT for the 3d–4f pair is particularly scarce. There is a study on the calculation of J for a Cu–Gd pair but as the authors employed a pure functional which has been proven to provide poor reproduction of the J values (both in magnitude and the sign), the computation provided the wrong sign for J.[6,35] To circumvent the issues related to the DFT methods, the straightforward way would be to employ highly correlated *ab initio* methods such as CASSCF and CASPT2 or DDCI (difference dedicated CI method which is particularly developed to obtain accurate energy differences between spin states[36]). However, these calculations are very time consuming and are hugely demanding beyond binuclear units with more than one unpaired electron per centre. A pioneering CASSCF study on a Cu–Gd pair[5] is available and, as expected, this method provided a very good numerical estimate of J and additionally demonstrated the fact that the 5d orbitals of the Gd are responsible for the intrinsic ferromagnetic coupling observed in the Cu–Gd pair.

Here we have employed DFT calculations on the full structure of $[L^1CuGd(O_2CCF_3)_3(C_2H_5OH)_2]$ (**1**) (See Fig. 1) to compute the magnetic exchange between the two metal atoms. In **1** the Cu(II) and the Gd(III) atoms are separated by 3.391 Å. The two metal ions are bridged by two phenoxo oxygens belonging to the ligand with angles of 103.2 and 103.4° and also by a carboxylate ligand. The O–Cu–O–Gd dihedral angle is found to be 11.5° revealing a significant twist from planarity. The calculation on **1** yields the J value as -5.9 cm^{-1}, revealing a ferromagnetic interaction between the Cu(II) and the Gd(III) ions and this is in excellent agreement with the experimental value of -4.42 cm^{-1}.

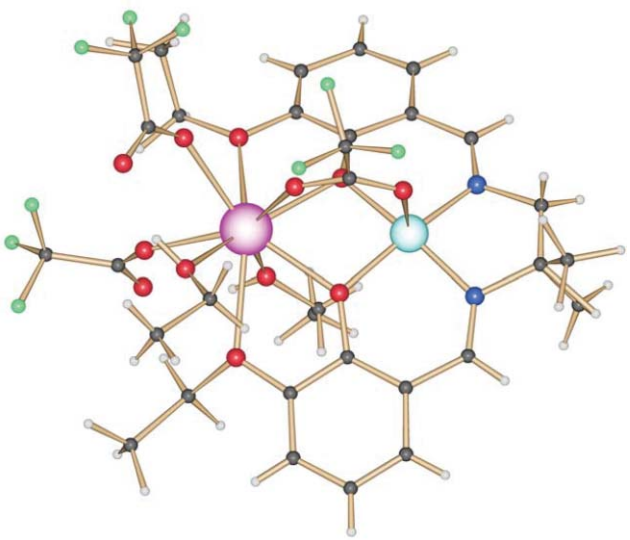

Fig. 1 The crystal structure of $[L^1CuGd(O_2CCF_3)_3(C_2H_5OH)_2]$ (**1**). The Gd(III) in pink, Cu(II) in cyan, Oxygen in red, fluorine in green and nitrogen in blue.

3.2. Method assessment for the computation of the J value

As previous theoretical studies using a pure density functional have been shown to provide the wrong sign for J[6,35] we have tested some hybrid and non-hybrid functionals with a variety of local and exchange correlations in order to assess a suitable functional for the studies on molecules containing the rare earth ions. For the evaluation of suitable functionals, several GGA, meta-GGA and hybrid functionals with varying percentages of HF exchange have been performed and the results are summarised in Table 1 (see ESI for a detailed discussion regarding the employed functionals†). The overview of the table suggests that the magnitude of J decreases when the percentage of HF exchange increases independent of the nature of the exchange and the correlation functional employed and that the performance of both the hybrid and the half-and-half functionals is satisfactory. Since no significant improvement is obtained with the modified exchange or correlation functionals, we have performed all the calculations with the hybrid B3LYP functional and we recommend the use of B3LYP for studies on similar systems.

We have also tested the basis set stability for the evaluation of J and the results are summarised in Table 2. The basis sets employed fall into mainly two categories: one set contains ECP for the Cu and the Gd atoms while the other set contains all electron basis set for all atoms. For all electron basis sets, calculations have been performed with and without incorporating the relativistic effects either *via* DKH or ZORA methods. All ten different basis set combinations tested yield a ferromagnetic J constant. The incorporation of the relativistic effects either *via* the ECP method or *via* the all electron DKH/ZORA method yields a good estimate of J (in the range of -5.2 to -5.8 cm^{-1}). However, if the relativistic effects were completely ignored the estimated J values were slightly higher. This demonstrates that the use of either an ECP basis set or an all electron basis set incorporating some relativistic contributions is necessary for studies on such systems.

3.3. Mechanism of magnetic coupling

Most of the Gd(III)–Cu(II) complexes and also the [Gd(III)Cu(II)] units in polynuclear complexes exhibit ferromagnetic interactions.[37–40] Although the magnitude of the J values varies across different structures, the variations are very minimal and stay in the weak ferromagnetic region in all cases except in one example where the antiferromagnetic interaction was perceptible.[9] The overall picture suggests that there is rather a general mechanism of exchange that applies for this pair. To obtain insight into the mechanism of coupling, several schematic pathways have been put forth.[42] A summary of the proposed schemes is as follows: since the $4f^7$ orbitals of the Gd(III) are contracted around the nucleus and they are efficiently shielded by the 5s and 5p occupied orbitals they do not interact directly with the oxygen orbitals of the ligand and therefore a direct super-exchange mechanism with the Cu(II) 3d orbitals with that of the 4f is negligible.

Previous experimental work by our group[38–41] and of Kahn[42–44] put forward an alternative polarisation mechanism where there is a

coupling between the 3d metal ground state configuration and that of the metal–metal charge transfer configuration. The excitation takes place from the singly-occupied copper orbital to either the empty 5d or 6s orbital of the Gd(III) as proposed by Kahn and Gatteschi, respectively. Since the 5d orbitals are very diffuse they are likely to be delocalised on the bridging oxygen atoms thus promoting the exchange interaction between the two metals. The reported CASSCF calculations revealed that the exclusion of the 5d orbital from the active space (containing only the 5d+4f+6s orbitals) yielded an extremely small ferromagnetic coupling and incorporation of the 5d orbital into the active space was necessary to reproduce the experimental J value.[5] This suggests that the role of the 6s shell on the magnetic coupling is rather small.

In order to obtain insight into the orbital ordering and the magnetic coupling, we have analysed the DFT wave function. The alpha spin MOs obtained from our DFT calculations of the high spin state are plotted in Fig. 2. The occupied and the empty orbitals having significant Gd and Cu contributions were picked up from the ladder and plotted separately in the figure for clarity. It is clear from the figure that the $4f^7$ orbitals of the Gd(III) are very low in energy (*ca.* 1000 kJ mol^{-1} lower from the Cu magnetic orbital) and are well localised on the Gd centre (see Fig. 3a–g). There are a few other MOs closer in energy to the copper $d_{x^2-y^2}$ type magnetic orbital and these orbitals have predominant d- and s- character on the Gd. They are shown in the figure as Gd-5d and Gd-6s. Apparently the Gd-5d orbitals are closer in energy and hence likely to play a predominant and a crucial role in the magnetic coupling. Additionally, the spin density distribution of the high spin state (see Fig. 3i) confirms the polarisation mechanism operating in this complex. The spin density on the Cu(II) (0.597) is delocalised to other atoms while in the Gd(III) (7.027) the unpaired electrons are fully localised on the Gd and a slight increase in the spin density is due to the spin polarisation mechanism. The two nitrogen atoms coordinated to the Cu(II) and the two bridging oxygen atoms have positive spin densities (0.132 and 0.129 on the nitrogens and 0.075 and 0.074 on the oxygens) due to predominant delocalisation mechanisms.[45]

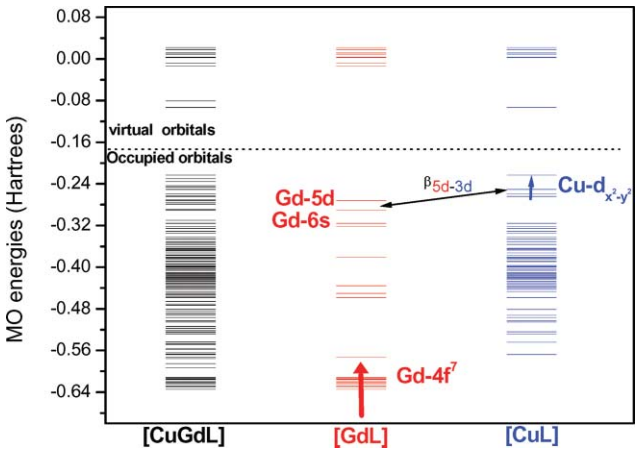

Fig. 2 The MO order of alpha MOs in **1** using the B3LYP/CSDZ method. The [GdL] and the [CuL] are picked from the ladder and represent the MOs having significant contributions from the two atoms. The blue and the red arrows indicate the approximate location of unpaired electrons. Note that in the [CuL] orbitals, the Cu-$d_{x^2-y^2}$ orbital is not the HOMO. The double headed arrow and the charge transfer integral $\beta_{5d\text{-}3d}$ denote the charge transfer between the two orbitals.

The oxygen atoms coordinated to the Gd have small negative spin density due to the predominant spin polarisation mechanism (from –0.001 to –0.003). A smaller spin density value found on the bridging oxygens (~0.07), compared to that

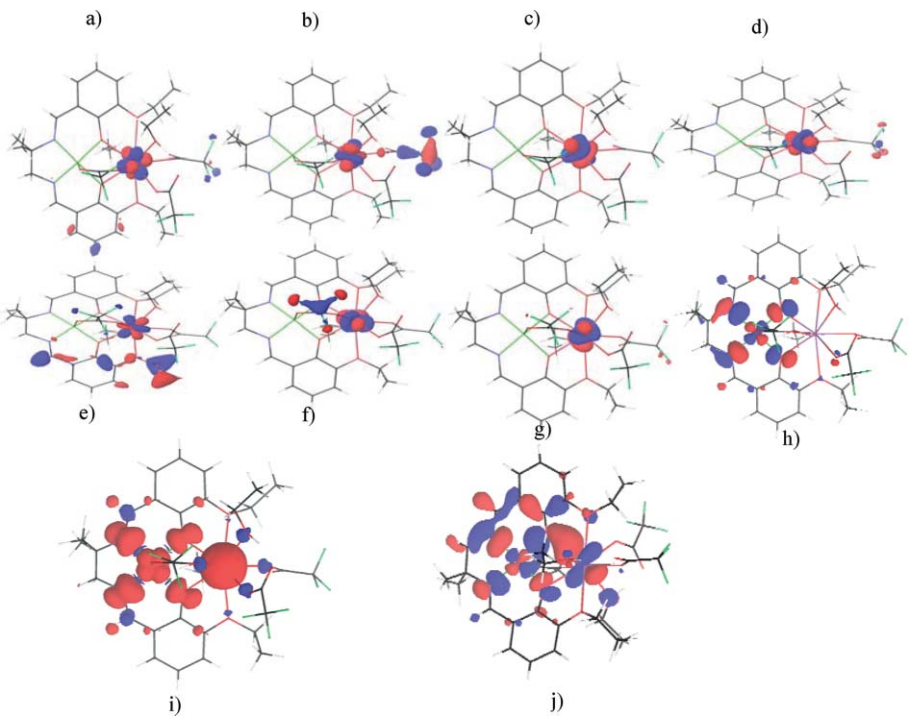

Fig. 3 a)–g) The alpha MOs of the $4f^7$ of the Gd(III), h) $3d_{x^2-y^2}$ of the Cu(II), i) the spin density distribution on **1**, j) a sample MO artificially magnified by suppressing the ligand contributions to clearly visualise the 5d orbitals of the Gd(III) to which the Cu(II) is associated in charge transfer phenomena.

of nitrogen atoms (~0.13), is probably due to a competing spin delocalisation from the Cu and spin polarisation from the Gd atoms. Further, the natural bond orbital (NBO) analysis revealed the electronic configuration of the Gd(III) as [core electrons]6s(0.23)4f(7.01)5d(0.13)6p(0.01), thus the spin on the 4f electrons is closer to the expected value of 7.00 while the 5d and 6s orbitals also have significant contributions despite being empty orbitals.

The five 5d orbitals of the Gd(III) in the NBO analysis appeared as a Rydberg anti-bonding orbitals (these are the empty high-lying orbitals with significant fractional occupation) (see Table S1 in ESI†). The hybridisation coefficients on these five 5d orbitals of **1** reveal some interesting insights: the f orbital coefficients on the 5d hybridisation are of two sets, two lower values (belongs to σ-type orbitals) and three higher values. This suggests that the two lower value orbitals gain density probably *via* the charge transfer (CT) from the Cu(II) $3d_{x^2-y^2}$ orbital and the other three orbitals are likely to gain predominant density *via* the 4f delocalisation. This picture has also been visualised from the NBO analysis on other model complexes discussed below. Some of the ligand MOs having the Cu $3d_{x^2-y^2}$ character have the f orbitals' wave function tail on the Gd centre. In **1** there are two types of f orbital found to have significant coefficient of the Gd(III) with the Cu(II) orbitals (this means an overlap of the $d_{x^2-y^2}$ orbital with the Gd(III) f orbital). In the approximate C_{2v} symmetry of the complex, the $4f^7$ orbitals transform as the following irreducible symmetry representations: $2a_1 + 2b_1 + 2b_2 + a_2$. The orbitals that have the wave function tail with the Cu(II) $d_{x^2-y^2}$ orbitals are of the $2b_2$ type (see Fig. 3j). Since the Cu(II) $d_{x^2-y^2}$ orbital transforms as b_2, this suggests that there are two interactions responsible for the antiferromagnetic coupling in this complex as also evidenced in the previous CASSCF studies.[5]

To gain further understanding of the magnetic coupling, a breakdown approach has been followed, whereby calculations have been performed on several model complexes of **1** in order to have an in-depth view on the multiple contributions to the net exchange interaction. These calculations are summarized in Table 3. The presence of a 3d element which matches the energies of the 5d orbitals of the Gd(III) is necessary for an efficient coupling. If this atom is replaced by another Gd(III) ($[L^1Gd(\mu\text{-}O_2CCF_3)Gd(O_2CCF_3)_2(C_2H_5OH)_2]^+$) the exchange interaction is then expected to be weak. In fact, calculations on such a model complex, **1a**, yielded an antiferromagnetic J (0.55 cm^{-1}). The complementary or counter-complementary effects[44,46] in **1** (model **1b**) have been analysed by eliminating the role of carboxylates and modelling them, instead, as two water molecules. The computed J value of −5.8 cm^{-1} suggests that the bridging carboxylates do not play any significant role on the coupling and this was also expected since the $d_{x^2-y^2}$ orbital of Cu(II) lies orthogonal to the axial ligand. The role of the oxygen bridge is better understood with model **1c** where one of the bridging oxygen atoms is replaced by a hydrogen atom. In this model, the interaction becomes antiferromagnetic ($J = 4.5$ cm^{-1}), demonstrating that the Cu–Gd interaction is not intrinsically ferromagnetic but can well be antiferromagnetic when the bridging moieties are altered. (Note the exchange pathways available for **1c** are (i) one extended Cu–N–CCCC–O–Gd path and (ii) one *via* the oxygen bridge). This is consistent with the experimental findings where antiferromagnetic J has been observed for a [CuGd] complex possessing different bridging groups[9] compared to **1**.

Table 3 The B3LYP computed J values on different model structures

Model structure	Models	DFT J/cm^{-1}
$[L^1Cu(\mu\text{-}O_2CCF_3)Gd(O_2CCF_3)_2(C_2H_5OH)_2]$	**1**	−5.9
$[L^1Gd(\mu\text{-}O_2CCF_3)Gd(O_2CCF_3)_2(C_2H_5OH)_2]^+$	**1a**	0.55
$[L^1Cu(H_2O)_2Gd(O_2CCF_3)_2(C_2H_5OH)_2(H_2O)_2]^+$	**1b**	−5.8
$[L^{1a}Cu(H_2O)_2Gd(O_2CCF_3)_2(C_2H_5OH)_2(H_2O)_2]^{2+}$	**1c**	4.5

L^{1a}- One of the bridging oxygen atom in the L^1 is replaced by a hydrogen atom.

The overall mechanism for the magnetic coupling can be understood from the different perspectives obtained from the above arguments and evidence. A schematic mechanism derived that fits well for the current situation is shown in Scheme 1.

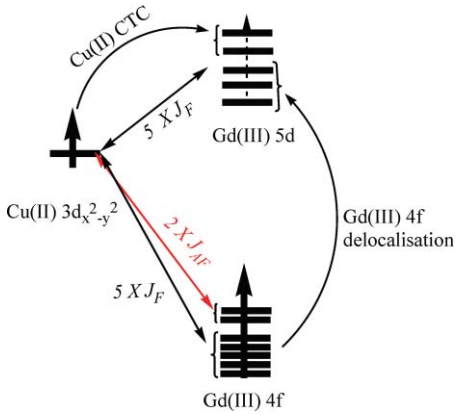

Scheme 1 A schematic mechanism for the magnetic coupling on the [GdCu] pair obtained from the DFT calculations. The nature and the number of interactions between the Cu(II) and the Gd(III) are shown by double headed arrows. The Gd(III) 5d orbitals gain density *via* the Cu(II) charge transfer and also *via* the 4f delocalisation.

The interaction between the Cu(II) 3d and the Gd(III) 5d contribute to the ferromagnetic part of the total exchange while the interaction of the Cu(II) with that of the Gd(III) $4f^7$ has two contributions: two orbitals that overlap with the $d_{x^2-y^2}$ orbital contribute to antiferromagnetic term while the rest of the five orbitals, being orthogonal, give rise to the ferromagnetic contribution to the total J. The net interaction is therefore ferromagnetic and, since none of the interaction terms derived are first order effect, the overall magnitude of the exchange is very small.

With this picture in mind, if we consider the interaction in the model **1a**, the weak antiferromagnetic interaction found in the [GdGd] dimer can be rationalised. In this case, the $4f^7$–$4f^7$ interaction term (possibly *via* the wave function tail on the 5d orbitals) will contribute to the antiferromagnetic coupling while the diminished 5d–5d would contribute to the ferromagnetic term resulting in a net antiferromagnetic interaction. Note that antiferromagnetic [GdGd] dimers with very small J values have been reported.[47] Now, in the extreme cases, for example in the model **1c**, the interaction becomes antiferromagnetic. This is essentially due to the loss of symmetry and hence the Cu(II) orbitals can eventually overlap with all the $4f^7$ orbitals contributing only to the antiferromagnetic part (see Fig. S1 of the ESI† where MOs with significant Cu(II) and Gd(III) coefficients are

plotted). Additionally the 5d–3d ferromagnetic contribution also drops significantly compared to that of **1**, due to inefficient charge transfer from the Cu(II). (This is supported by the fact that the NBO coefficients on the two 5d orbitals, which are due to the charge transfer from the Cu(II), have been significantly reduced.)

Now we turn to other 3d–4f systems to see if this picture still holds. For example, in the case of a Cr(III)Gd(III) pair, a ferromagnetic contribution 3d–5d (expected to be less efficient due to the presence of unpaired spins in the t_{2g} type orbitals in the Cr(III) and thus a diminished CT to the 5d orbitals of the Gd(III)) and a competing antiferro–ferro magnetic interaction results. As the number of possible overlaps between the two sets of magnetic orbitals increases compared to those of the [GdCu] pair, the net interaction is predicted to be antiferromagnetic. This is in good agreement with the experimental finding where the Cr(III)Gd(III) interactions are found to be overwhelmingly antiferromagnetic,[48] demonstrating the general applicability of our mechanism to the 3d–4f complexes.

3.4. Magneto-structural correlations

The magneto-structural correlations are important means to interpret the observed magnetic properties of novel and/or more complex compounds to design new compounds with expected magnetic properties. Since several dinuclear and polynuclear complexes containing the [CuGd] building blocks have been reported so far, two magneto-structural correlations have been developed based on the available data. Focusing on the [CuGd] structural parameters, the first correlation proposed by Winpenny *et al.*[10] suggests a dependence on the Gd–Cu distance while the second correlation proposed by Costes *et al.*[11] relates the dihedral angle between the CuO_2 and the GdO_2 plane. The [Cu···Gd] distance correlation was found to be related by an exponential function:

$$J = Ae^{[Bd_{Gd\text{-}Cu}]},$$

where $A = 6.409 \times 10^4$ and $B = -2.833$ and $d_{Gd\text{-}Cu}$ is [Cu···Gd] distance. However this correlation is found to be inadequate to account for *ca.* $J > 8$ cm^{-1}. Consequently a second correlation incorporating further experimental data was proposed to relate the J value to the dihedral angle (α) between the CuO_2 and GdO_2 planes with an exponential dependence,[11]

$$|J| = Ae^{[B\alpha]},$$

where $A = 11.5$ and $B = -0.054$. Both correlations, however, have been developed based on the analysis of a limited number of experimental data and therefore do not appear to be completely reliable.[11] Initially, with the DFT calculations, we have been able to develop magneto-structural correlations on **1** by varying the [Cu···Gd] distance. The correlations have been done mainly in the model complex **1b** as the presence of rigid carboxylate bridges in the full structure of **1** prevents a particular structural variation and also their influence on the magnitude of the J values is negligible. In the model **1b** the variations of [Cu···Gd] distance result in the variation of the Cu–O–Gd angle as well, so two parameters have been varied at the same time. The correlation found by varying the Cu–O–Gd angle from 90 to 116° (or the [Cu···Gd] distance from 2.3 to 4.8 Å) is shown in Fig. 4a. The correlation has the shape of

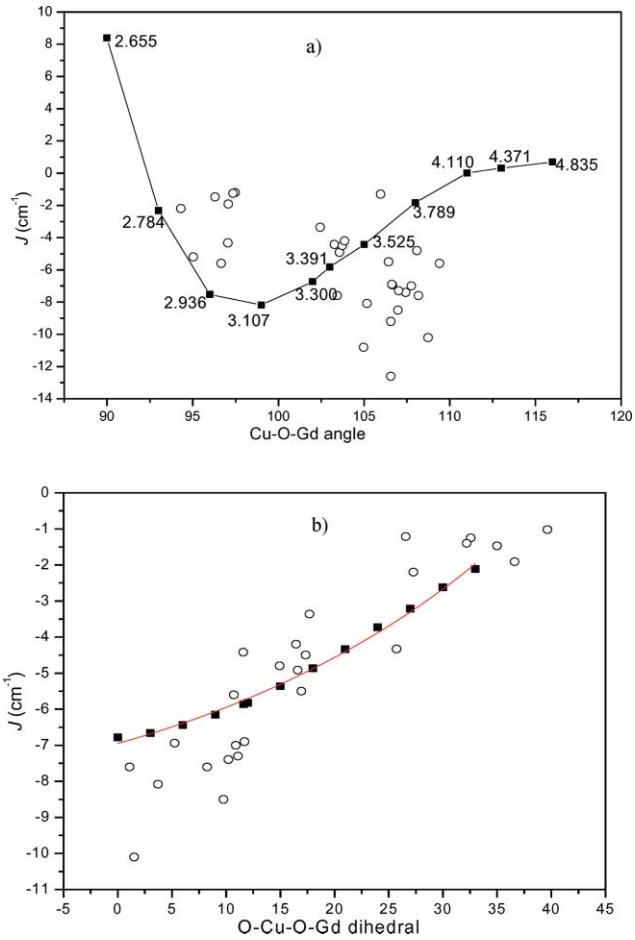

Fig. 4 Magneto-structural correlations developed by DFT calculations (B3LYP/CSDZ) by varying the structural parameters a) Gd–O–Cu angle (or [Gd···Cu] distance, and b) O–Cu–O–Gd dihedral angle on **1**. The open circles represent the experimental points obtained from the crystal structure and J from the magnetic susceptibility measurements. The red line on graph b) is the exponential growth fit for the DFT points. (R^2 = 0.9958).

the Morse curve, and reveals an antiferromagnetic interaction at lower angles (Cu–O–Gd angle >93° or [Cu···Gd] >2.7 Å).

On increasing the angle, the J value becomes more ferromagnetic exhibiting a maximum strength at an angle of 99°, then it decreases and approaches zero for Cu–O–Gd angle >110°. The anti-ferromagnetic interaction occurring at an acute angle is due to the inefficient charge transfer from the Cu(II) to the 5d orbitals of the Gd(III) and an increased overlap between the magnetic orbitals. The spin density values of the Gd(III) and of the Cu(II) plotted against the angle are shown in Fig. 5a. The spin densities on both centres increase with the increase in the angle up to the value of 103°. Afterwards, the Gd(III) shows a plateau while the Cu(II) spin density decreases. The increase in spin density means less delocalisation and this correlates with the increase in ferromagnetic coupling observed in Fig. 4a. The experimental J values for 26 different [CuGd] dinuclear complexes plotted (see Table S2 in the ESI†) along with the DFT correlation shows rather a scattered picture (also for the [Cu···Gd] distance). This suggests either the [Cu···Gd] distance or the angle is not a

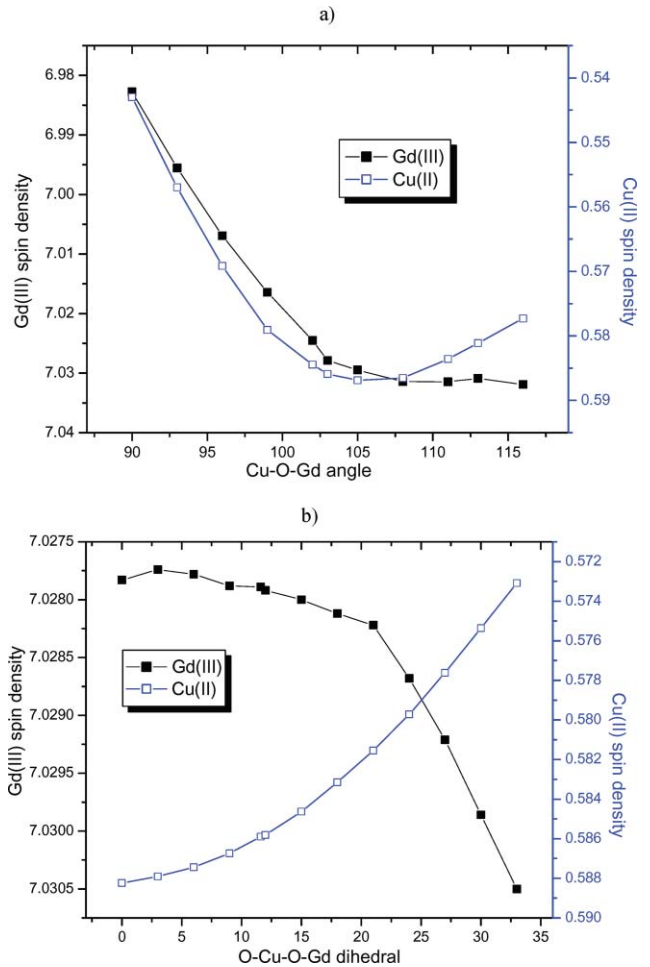

Fig. 5 The spin density variation in the Cu(II) and Gd(III) for $S_T = 4$ of **1** along the magneto-structural correlation parameters a) the Gd–O–Cu angle (or [Gd···Cu] distance, and b) the O–Cu–O–Gd dihedral angle.

unique parameter which determines the magnitude (and also the sign) of the exchange coupling.

Therefore, another correlation has been developed by varying the CuO_2 and GdO_2 dihedral angle on the model **1b** from 0 to 33°. This gives an exponential relationship with J where increasing the dihedral angle decreases the magnitude of J (see Fig. 4b). Fitting the data for an exponential growth equation yielded the following equation,

$$J = A + Be^{(\alpha/t)},$$

where $A = -9.599$, $B = 2.651$, $t = 31.20455$ and α is the torsion angle.

In this case, the experimental data are less scattered revealing that this correlation is perhaps more reliable than the previous ones. It is also important to note that the collected experimental structures of the dinuclear complexes contain the [GdO_2Cu] moiety and in some cases other bridging ligands are also present. Additionally, while the dihedral is varied, it is also likely that this will change the [Gd···Cu] distance or the Cu–O–Gd angle. This correlation predicts a ferromagnetic to antiferromagnetic switch at $\alpha = 40.5°$ and this strikingly correlates with the antiferromagnetic interaction reported for the [GdCu] complexes with α ranging from 40 to 46°.[9] The spin density plot reveals an interesting twist—since the ferromagnetic interaction decreases when the dihedral angle increases, the spin density is expected to decrease leading to more delocalised spins on the metal centres. The Cu(II) spin density correlates with this idea (its spin density decreases with the decrease in ferromagnetic J). However the Gd(III) spin density behaves differently: it is nearly constant for up to the value of 21° and then its spin density increases monotonically. This suggests that at higher dihedral values the role of the Gd(III) becomes prominent in keeping J within the ferromagnetic region.

4. Conclusions

Despite extensive experimental studies and some pioneering theoretical work, the [GdCu] coupling is still an intriguing problem. Several theoretical issues related to the method assessment and the mechanism of coupling still remain elusive. With the state-of-the art DFT calculations in hand we have attempted to shed some light on these issues by offering (i) suitable method to study such complexes within the DFT formalism, (ii) a profound insight into the mechanism of coupling and (iii) a reliable magneto-structural correlation which has potential applications beyond dinuclear units.

The DFT calculations are robust compared to any highly correlated *ab initio* methods and are often employed for studies on very large molecules. In this regard the method assessment presented in the first section is important—although the conclusions obtained are not unusual compared to that of transition metal complexes. A dependency of J values on the % of HF exchange has been observed while testing with both the popular functionals as well as the recently reported new functionals. The results suggest that there is no significant improvement over the use of the standard hybrid functionals and, accordingly, the application of the favourite B3LYP functional is still enduring. An extensive test performed to check the basis set stability for computation of J reveals that the relativistic effects are important for a good estimate of J—this can be done using either an ECP basis set or by incorporating the relativistic contribution by DKH/ZORA with an all electron basis set.

The second issue regarding the mechanism of coupling is indispensable. The two schematic mechanisms proposed based on the experimental studies are highly valuable but contradict each other on which empty orbital (5d or 6s) of the Gd(III) has a pronounced role on the magnetic coupling. The mechanistic insights derived here are not solely from our DFT calculations but we have also made use of the pioneering CASSCF studies on this system reported earlier.[5] Both methods suggest that the 5d orbitals of the Gd(III) have a predominant role on the coupling. The observation from our calculations is that the 5d orbitals not only gain density *via* the charge transfer from the 3d counterpart (in this case the Cu(II)) but also due to the half filled 4f orbitals. This is not surprising given the fact that the 5d orbitals are more diffuse and the calculated radial charge densities on the Gd atom reveal a significant overlap with that of the 4f. This yields a strong direct exchange to the 5d orbitals.[49] We have also found that only two of the 5d orbitals gain density *via* the charge transfer from the Cu(II) while other three orbitals predominantly gain density due to the 4f. The presence of the unpaired electron in a σ-type orbital in the 3d element is rather crucial for an efficient charge transfer. Apart from this, the

symmetry of the complex plays an important role on the coupling. In fact the magnetic orbital of Cu(II) has the wave function tail on only two of the 4f (due to symmetry restrictions) suggesting an antiferromagnetic contribution while the other five 4f orbitals remain orthogonal, providing a ferromagnetic contribution. The net interaction arising from the competition between all these contributions has the number of ferromagnetic terms dominating, leading to a negative *J*. This mechanism can be used to rationalise the antiferromagnetic *J* found in the [GdCu] complexes with a very large O–Cu–O–Gd dihedral angle (experimental) or an acute Cu–O–Gd angle. Therefore this mechanism has rather a general applicability. The role of the 6s orbital on the coupling is found to be small despite having significant spin density. Nevertheless, we believe that the 6s orbital is not entirely innocent and could have a vital role in polynuclear complexes (for example Cu(II)–Gd(III)–Cu(II) trinuclear complexes). Experimentally it has been found that the Gd(III) 5d orbitals have no significant role on the next-nearest neighbour interaction in the polynuclear complexes.[50] The possible involvement of other orbitals, particularly the 6s, on the next-nearest neighbour interaction is an attractive idea and we are currently working on this issue.

The magneto-structural correlations developed here suggest that the O–Cu–O–Gd dihedral angle is a more reliable parameter than [Cu · · · Gd] distance or Cu–O–Gd angle. The dependence of *J* on the structural parameters is rationalised using the spin density distribution on the Cu(II) and Gd(III) atoms.

Acknowledgements

G.R. would like to thank the European Union for the Marie Curie Incoming International fellowship. We would like to thank Prof. Eliseo Ruiz, University of Barcelona, Spain, for providing us with the contracted version of the all electron Gd basis set.

References

1 R. Sessoli, D. Gatteschi, A. Caneschi and M. A. Novak, *Nature*, 1993, **365**, 141; G. Christou, D. Gatteschi, D. N. Hendrickson and R. Sessoli, *Mater. Res. Bull.*, 2000, **25**, 66.
2 L. Bogani, C. Sangregorio, R. Sessoli and D. Gatteschi, *Angew. Chem., Int. Ed.*, 2005, **44**, 5817.
3 C. Aronica, G. Pilet, G. Chastanet, W. Wernsdorfer, J.-F. Jacquot and D. Luneau, *Angew. Chem. Int. Ed.*, 2006, **118**, 4775; A. Mishra, W. Wernsdorfer, K. Abboud and G. Christou, *J. Am. Chem. Soc.*, 2004, **126**, 15648; A. Mishra, W. Wernsdorfer, S. Parsons, G. Christou and E. K. Brechin, *Chem. Commun.*, 2005, **16**, 2086; V. Mereacre, A. Ako, R. Clerac, W. Wernsdorfer, G. Filoti, J. Bartolome, C. E. Anson and A. K. Powell, *J. Am. Chem. Soc.*, 2007, **129**, 9248.
4 J. P. Costes, M. Auchel, F. Dhan, V. Peyrou, S. Shova and W. Wernsdorfer, *Inorg. Chem.*, 2006, **45**, 1924.
5 J. Paulovic, F. Cimpoesu, M. Ferbinteanu and K. Hirao, *J. Am. Chem. Soc.*, 2004, **126**, 3321.
6 F. Yan and Z. D. Chen, *J. Phys. Chem. A*, 2000, **104**, 6295.
7 I. Rudra, C. Raghu and S. Ramasesha, *Phys. Rev. B*, 2002, **65**, 224411.
8 G. Novitchi, S. Shova, A. Caneschi, J. P. Costes, M. Gdaniec and N. Stanica, *Dalton. Trans.*, 2004, 1194.
9 J. P. Costes, F. Dahan, A. Dupuis and J. P. Laurent, *Inorg. Chem.*, 2000, **39**, 169; J. P. Laurent, F. Dahan and A. Dupuis, *Inorg. Chem.*, 2000, **39**, 5994.
10 C. Benelli, A. J. Blake, P. E. Y. Milne, J. M. Rawson and R. E. P. Winpenny, *Chem.–Eur. J.*, 1995, **1**, 614.
11 J. P. Costes, F. Dahan and A. Dupuis, *Inorg. Chem.*, 2000, **39**, 165.
12 L. Noodleman, *J. Chem. Phys.*, 1981, **74**, 5737.
13 E. Ruiz, S. Alvarez, J. Cano and P. Alemany, *J. Comput. Chem.*, 1999, **20**, 1391; E. Ruiz, A. R. Fortea, J. Cano, S. Alvarez and P. Alemany, *J. Comput, Chem.*, 2003, **24**, 982; E. Ruiz, J. Cano, S. Alvarez, A. Caneschi and D. Gatteschi, *J. Am. Chem. Soc.*, 2003, **152**, 6791; G. Rajaraman, J. Cano, E. K. Brechin and E. J. L. McInnes, *Chem. Commun.*, 2004, 1476; P. Christian, G. Rajaraman, A. Harrison, J. J. W. McDouall, J. Raftery and R. E. P. Winpenny, *Dalton. Trans.*, 2004, 2550; G. Rajaraman, M. Murugesu, E. C. Sanudo, M. Soler, W. Wernsdorfer, M. Helliwell, C. Muryn, J. Raftery, S. J. Teat, G. Christou and E. K. Brechin, *J. Am. Chem. Soc.*, 2004, **126**, 15445; A. Bencini and F. Totti, *Int. J. Quantum Chem.*, 2005, **101**, 819; K. Hegetschweiler, B. Morenstern, J. Zubieta, P. J. Hagrman, N. Lima, R. Sessoli and F. Totti, *Angew. Chem., Int. Ed. Engl.*, 2004, **43**, 3436.
14 C. Adamo, V. Barone, A. Bencini, F. Totti and I. Ciofini, *Inorg. Chem.*, 1999, **38**, 1996.
15 *JAGUAR 7.0 Schrödinger, Inc.*, Portland, 2007.
16 A. D. Becke, *J. Chem. Phys.*, 1993, **98**, 5648.
17 T. R. Cundari and W. J. Stevens, *J. Chem. Phys.*, 1993, **98**, 5555.
18 T. H. Dunning, Jr. and P. J. Hay, in *Modern Theoretical Chemistry*, ed. H. F. Schaefer, III, vol. 3, Plenum, New York, 1976, 1–28; P. J. Hay and W. R. Wadt, *J. Chem. Phys.*, 1985, **82**, 270.
19 R. Ditchfield, W. J. Hehre and J. A. Pople, *J. Chem. Phys.*, 1971, **54**, 724; V. A. Rassolov, M. A. Ratner, J. A. Pople, P. C. Redfern and L. A. Curtiss, *J. Comput. Chem.*, 2001, **22**, 976.
20 D. Feller, *J. Comp. Chem.*, 1996, **17**, 1571.
21 K. L. Schuchardt, B. T. Didier, T. Elsethagen, L. Sun, V. Gurumoorthi, J. Chase, J. Li and T. L. Windus, *J. Chem. Inf. Comput. Sci.*, 2007, **47**, 1045.
22 L. E. Roy, P. J. Hay and R. L. Martin, *J. Chem. Theory Comput.*, 2004, **4**, 1029.
23 A. Bergner, M. Dolg, W. Kuechle, H. Stoll and H. Preuss, *Mol. Phys.*, 1993, **80**, 1431.
24 M. Dolg, H. Stoll, H. Preuss and R. M. Pitzer, *J. Phys. Chem.*, 1993, **97**, 5852.
25 M. M. Hurley, L. F. Pacios, P. A. Christiansen, R. B. Ross and W. C. Ermler, *J. Chem. Phys.*, 1986, **84**, 6840.
26 R. B. Ross, W. C. Ermler and S. Das, unpublished.
27 A. Schafer, C. Huber and R. Ahlrichs, *J. Chem. Phys.*, 1994, **100**, 5829.
28 A. J. H. Wachters, *J. Chem. Phys.*, 1970, **52**, 1033.
29 T. Nakajima and K. Hirao, *J. Chem. Phys.*, 2002, **116**, 8270.
30 E. V. Lenthe, E. J. Baerends and J. G. Snijders, *J. Chem. Phys.*, 1993, **99**, 4597.
31 M. Douglas and N. M. Kroll, *Ann. Phys.*, 1974, **82**, 89.
32 B. A. Hess, *Phys. Rev. A.*, 1985, **32**, 756.
33 *Gaussian 03*, Revision C.01, M. J. Frisch, G. W. Trucks, H. B. Schlegel, G. E. Scuseria, M. A. Robb, J. R. Cheeseman, J. A. Montgomery, Jr., T. Vreven, K. N. Kudin, J. C. Burant, J. M. Millam, S. S. Iyengar, J. Tomasi, V. Barone, B. Mennucci, M. Cossi, G. Scalmani, N. Rega, G. A. Petersson, H. Nakatsuji, M. Hada, M. Ehara, K. Toyota, R. Fukuda, J. Hasegawa, M. Ishida, T. Nakajima, Y. Honda, O. Kitao, H. Nakai, M. Klene, X. Li, J. E. Knox, H. P. Hratchian, J. B. Cross, V. Bakken, C. Adamo, J. Jaramillo, R. Gomperts, R. E. Stratmann, O. Yazyev, A. J. Austin, R. Cammi, C. Pomelli, J. W. Ochterski, P. Y. Ayala, K. Morokuma, G. A. Voth, P. Salvador, J. J. Dannenberg, V. G. Zakrzewski, S. Dapprich, A. D. Daniels, M. C. Strain, O. Farkas, D. K. Malick, A. D. Rabuck, K. Raghavachari, J. B. Foresman, J. V. Ortiz, Q. Cui, A. G. Baboul, S. Clifford, J. Cioslowski, B. B. Stefanov, G. Liu, A. Liashenko, P. Piskorz, I. Komaromi, R. L. Martin, D. J. Fox, T. Keith, M. A. Al-Laham, C. Y. Peng, A. Nanayakkara, M. Challacombe, P. M. W. Gill, B. Johnson, W. Chen, M. W. Wong, C. Gonzalez and J. A. Pople, Gaussian, Inc., Wallingford CT, 2004.
34 Orca, 2.6–35, F. Neese, Bonn, 2007.
35 S. Gao, O. Borgmeier and H. Lueken, *Acta Phys. Pol., A*, 1996, **90**, 393.
36 J. Miralles, O. Castell, R. Caballol and J. P. Malrieu, *Chem. Phys.*, 1993, **172**, 33.
37 A. Bencini, C. Benelli, A. Caneschi, R. L. Carlin, A. Dei and D. Gatteschi, *J. Am. Chem. Soc.*, 1985, **107**, 8128.
38 C. Benelli, A. Caneschi, D. Gatteschi, O. Guillou and L. Pardi, *Inorg. Chem.*, 1990, **29**, 1750.
39 A. Bencini, C. Benelli, A. Caneschi, A. Dei and D. Gatteschi, *Inorg. Chem.*, 1985, **25**, 572.
40 D. Gatteschi, *Adv. Mater.*, 1994, **6**, 635; C. Benelli, A. Caneschi, D. Gatteschi and R. Sessoli, *J. Appl. Phys.*, 1993, **73**, 5333.
41 C. Benelli, A. Caneschi, A. Fabretti, D. Gatteschi and L. Pardi, *Inorg. Chem.*, 1990, **29**, 4153.

42 O. Kahn, O. Guillou, in *Reserach Frontiers in Magnetochemistry*, ed. C. J. O'Conner, World Scientific, Singapore, 1993, pp 179; O. Kahn, *Angew. Chem., Int. Ed. Engl.*, 1985, **24**, 834.

43 I. Ramada, O. Kahn, Y. Jeannin and F. Robert, *Inorg. Chem.*, 1997, **36**, 930; O. Guillou, P. Bergerat, O. Kahn, E. Bakalbassis, K. Boubekeur, P. Batail and M. Guillot, *Inorg. Chem.*, 1992, **31**, 110.

44 O. Kahn, *Molecular Magnetism*, VCH Publishers, New York, 1993.

45 J. Cano, E. Ruiz, S. Alvarez and M. Verdaguer, *Comments Inorg. Chem.*, 1998, **20**, 27.

46 E. Escriva, J. Garcia-Lozano, J. Martinez-Lillo, H. Nunez, J. Server-Carrio, L. Sato, R. Carrasco and J. Cano, *Inorg. Chem.*, 2003, **42**, 8328.

47 L. E. Roy and T. Hughbanks, *J. Am. Chem. Soc.*, 2005, **128**, 568; L. E. Sweet, L. E. Roy, F. Meng and T. Hughbank, *J. Am. Chem. Soc.*, 2006, **128**, 10193; S. Liu, L. Gemini, S. J. Rittig, R. C. Thompson and C. Orvig, *J. Am. Chem. Soc.*, 1992, **114**, 6081; W. Plass and G. Z. Fries, *Z. Anorg. Allg. Chem.*, 1997, **623**, 1205.

48 R. Gheorghe, P. Cucos, M. Andruh, J.-P. Costes, B. Donnadieu and S. B. Shova, *Chem.–Eur. J.*, 2006, **12**, 187; H.-Z. Kou, B. C. Zhou and R.-J. Wang, *Inorg. Chem.*, 2003, **42**, 7658.

49 J. Stohr and H. C. Siegmann, *Magnetism From Fundamentals to Nanoscale Dynamics*, Springer, Heidelberg, Germany, 2006, pp 532.

50 G. Champion, N. Lallioti, V. Tangoulis, M.-A. Arrio, P. Sainctavit, F. Villain, A. Caneschi, D. Gatteschi, C. Giorgetti, F. Baudelet, M. Verdaguer and C. C. dit Moulin, *J. Am. Chem. Soc.*, 2003, **125**, 8371.